

# Composite LiFePO<sub>4</sub>/poly-3,4-ethylenedioxythiophene Cathode for Lithium-Ion Batteries with Low Content of Non-Electroactive Components

*O.V. Levin, S.N. Eliseeva, E.V. Alekseeva, E.G. Tolstopjatova, V.V. Kondratiev\**

Institute of Chemistry, St. Petersburg State University, 198504, St. Petersburg, Petrodvoretz, Universitetsky pr.26, Russian Federation

\*E-mail: [ykondratiev@mail.ru](mailto:ykondratiev@mail.ru), [elchem@chem.spbu.ru](mailto:elchem@chem.spbu.ru)

*Received:* 10 June 2015 / *Accepted:* 18 July 2015 / *Published:* 26 August 2015

---

Environmentally friendly and inexpensive olivine-type compound LiFePO<sub>4</sub> is one of the most promising cathode materials for lithium-ion batteries. Its poor electrical conductivity, however, requires introduction of large amounts of conductive carbon additives into LiFePO<sub>4</sub> - based cathode materials. The total content of conductive carbon additives and inactive polymeric binders reaches up to 15-20 wt.% of the mass of the electrode material. Therefore, one of the ways to increase electrode capacity is to reduce the amount of inactive components, in particular, by replacing them with conducting polymer. Here, we propose a new LiFePO<sub>4</sub> - based electrode composition comprising very high content (99.5 wt.%) of electroactive carbon-coated LiFePO<sub>4</sub> and a small amount (0.5 wt.%) of conducting polymer poly-3,4-ethylenedioxythiophene doped with polystyrene sulfonate (PEDOT:PSS), serving as a binder and conducting additive. Gravimetric energy density of these composite electrodes (147 mAhg<sup>-1</sup> at 0.2 C) is 15% higher than of conventional LiFePO<sub>4</sub> - based electrodes, while the cyclability and C-rate capability remains virtually at the same level.

---

**Keywords:** lithium iron phosphate; Li-ion batteries; PEDOT:PSS; C-rate capability; capacity

## 1. INTRODUCTION

Lithium iron phosphate LiFePO<sub>4</sub> (LFP) with the olivine structure is one of the leading candidates for production of environmentally friendly low-cost cathode materials for lithium-ion batteries with good performance and high energy and power density [1-3]. It has relatively high theoretical capacity (170 mAh g<sup>-1</sup>), but low ionic and electronic conductivity is the main drawback of this material. Recently it was shown that electrochemical performance of LFP can be significantly

enhanced through the improvement of the conductivity of the material. Different material preparation approaches, such as reducing the particle size [4-6], carbon coating [7-10], doping with transition metal ions [11-13], metal powder addition [14-15] were proposed.

The alternative approach to improve electronic conductivity of the active material is surface coating of LFP with conducting polymers, such as polyaniline, polypyrrole, polythiophene and its derivatives, showing a positive effect on electrochemical performance of LFP [4]. Among conducting polymers, poly-3,4-ethylenedioxythiophene (PEDOT) is especially attractive due to high electronic conductivity, chemical stability, mechanical flexibility, thermal stability and the ability to maintain Li-ion transport [2, 5-9]. Various methods were employed to prepare LFP/PEDOT composites with enhanced electrochemical performance [5, 6, 8, 10-12], including three phase interline electropolymerization of 3,4-ethylenedioxythiophene and LFP particles [19, 26], chemical polymerization of 3,4-ethylenedioxythiophene in the presence of LFP particles [20], casting of polymer colloidal suspension on LFP grains [17], casting of dispersion of poly-3,4-ethylenedioxythiophene doped with polystyrene sulfonate (PEDOT:PSS) onto pre-formed LFP or C-LFP electrode [27], mechanical mixing of PEDOT:PSS with LFP and non-conducting additives [27, 33].

Recently it was shown, that conducting polyelectrolyte dispersion PEDOT:PSS, which can act both as electron conducting additive and as a binder, turned out especially attractive, providing enhanced electrochemical performance of the electrodes [27, 33].

However, in the most cases of proposed LFP/PEDOT or LFP/PEDOT:PSS composites, large amounts either of carbon additives and inactive binders or conducting polymer were needed to produce mechanically stable electrodes with good electrochemical performance. Therefore, the values of capacities of LFP/PEDOT referred to the total weight of the composite electrodes including LFP and additives are relatively low (75–130 mAh g<sup>-1</sup> at 0.1 C) [16-18, 20, 27, 33].

Conventional cathode materials also contain large amounts (15–20 wt.%) of electron-conducting additives and inactive polymeric binders which do not contribute to the electrode capacity and thus reduce the energy and power density of the battery. Thus, one of important tasks is to improve practical storage capacity of the electrodes by minimizing the content of non-electrochemically active components (carbon and binder).

Attempts of straightforward replacement of traditional PVDF binder with large amount of conductive PEDOT:PSS blend, combined with elimination of other conductive additives (carbon black) have been made in [33]. The compositions of different wt.% of LiFePO<sub>4</sub> (94%, 92%, 84%) as active electrode material and corresponding wt.% of PEDOT:PSS (6%, 8%, 16%) as a binder material were tested. The composite electrodes with 8 wt.% PEDOT:PSS content, considered by authors as optimal ones, showed the best discharge capacities of about 120 mAhg<sup>-1</sup> at 0.2 C, which is comparable with traditional PVDF-bound electrodes [33].

Recently *Kim et al.* [31] reported a facile and cheap method for production of LiCoO<sub>2</sub> - based electrode from LiCoO<sub>2</sub> and PEDOT:PSS free of additional binders and conductive agents. It was called by the authors [31] a “monocomponent electrode”. It was demonstrated that in such case very thin films of polymer are covering active material particles, providing good electrical contact between them with a very short electron pathway length and thus a low electrode resistance.

We have extended this approach to produce for the first time C-LFP/PEDOT:PSS composite cathode material with 99.5 wt.% content of electrochemically active C-LFP. In this paper C-LFP/PEDOT:PSS composite cathode material with extremely low content of PEDOT:PSS was proposed and tested. In comparison to the electrodes with large amount of PEDOT:PSS (6-16 wt.%), proposed by other authors [33] electrodes obtained by us showed better specific capacity, prolonged cyclability and C-rate capability. In particular, specific discharge capacity of about  $147 \text{ mAhg}^{-1}$  at 0.2 C was obtained, which outperforms the values for traditional PVDF-bound electrodes and electrodes with large amounts of PEDOT:PSS [33].

## 2. EXPERIMENTAL

All reagents were used as received. Poly-3,4-ethylenedioxythiophene-polystyrene sulfonate (PEDOT:PSS) 1.3 wt.% aqueous dispersion, ethylene carbonate (EC), dimethyl carbonate (DMC),  $\text{LiPF}_6$ , polyvinylidene fluoride (PVDF) and N-methylpyrrolidone (NMP) were purchased from Aldrich. Commercial grade «P2» C- $\text{LiFePO}_4$  (C-LFP) was purchased from Phostech Lithium Inc. (Canada). Conductive carbon black «Super P» was purchased from Timcal Inc. (Belgium).

The composite cathode material was prepared by mechanical mixing of 99.5 wt.% C-LFP and 0.5 wt.% PEDOT:PSS followed by ultrasonification for 1h. The resulting viscous slurry was cast uniformly onto aluminium foil that served as a current collector, dried at  $80^\circ\text{C}$  under vacuum conditions and roll-pressed to achieve electrode active layer density  $2.6 \text{ g cm}^{-3}$ . For comparison the cathode material with conventional composition was prepared by mixing of 84 wt.% C-LFP, 8 wt.% carbon black and 8 wt.% of PVDF dissolved in NMP.

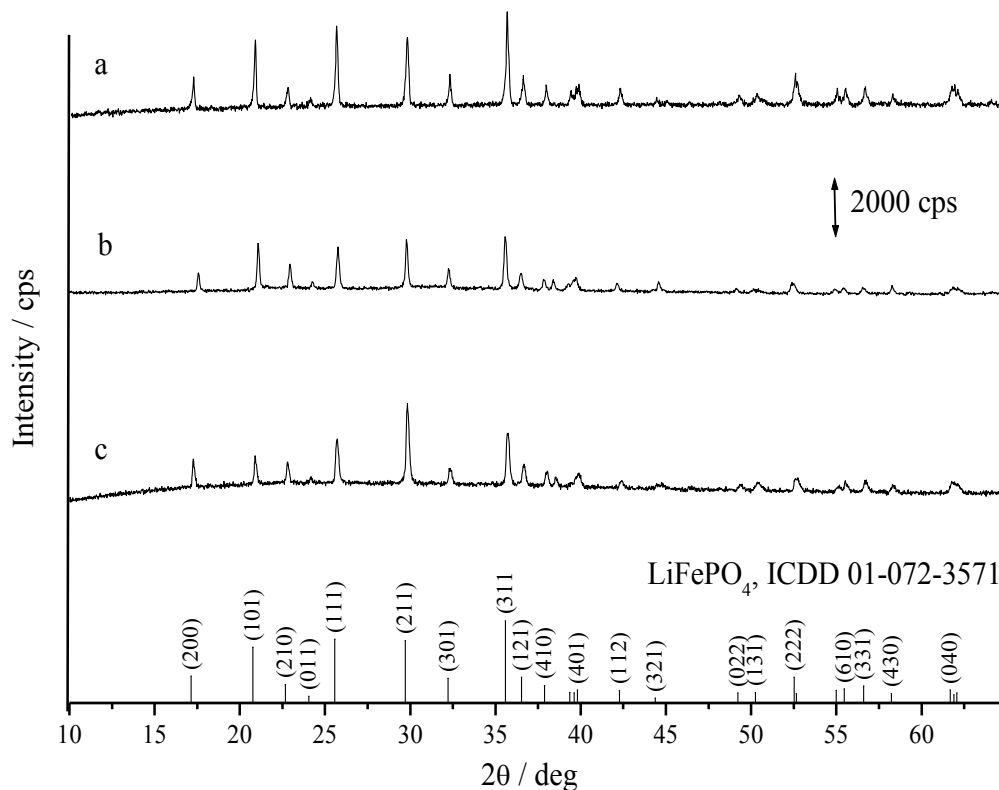
The morphology and structure of prepared composites were characterized by X-ray diffraction measurement (XRD, Bruker-AXS D8 DISCOVER using  $\text{Cu K}\alpha$  radiation) and scanning electron microscopy (SEM, SUPRA 40VP Carl Zeiss, Germany). EDX analysis was performed with an energy-dispersive X-ray spectrometer X-act (Oxford Instruments, United Kingdom).

The electrochemical characterization of the material was conducted in standard two-electrode coin-type half cells (CR2032). The test cells were assembled in an argon-filled glove box (Unilab, USA) using Celgard 2325 membrane as separator, 1 mol/L  $\text{LiPF}_6$  in a 1:1 (V:V) mixture of ethylene carbonate (EC) and dimethyl carbonate (DMC) as an electrolyte. The electrochemical performance tests were carried out on an automatic galvanostatic charge-discharge battery cell test instrument (Neware Co., China) in potential range between 2.0 and 4.0 V (vs.  $\text{Li/Li}^+$ ) under different current densities from 0.2 C to 5 C at room temperature ( $20 \pm 2^\circ\text{C}$ ). Battery charge was performed in constant current – constant voltage regime with cutoff current of constant voltage step equal to 0.01 C. 1 C current was calculated according to theoretical capacity of LFP  $170 \text{ mAh g}^{-1}$ . All capacity values, presented in the paper, were normalized by the total weight of electroactive materials. Electrochemical impedance spectroscopy (EIS) measurements were performed using an Autolab302 potentiostat-galvanostat (EcoChemie Instruments, The Netherlands).

### 3. RESULTS AND DISCUSSION

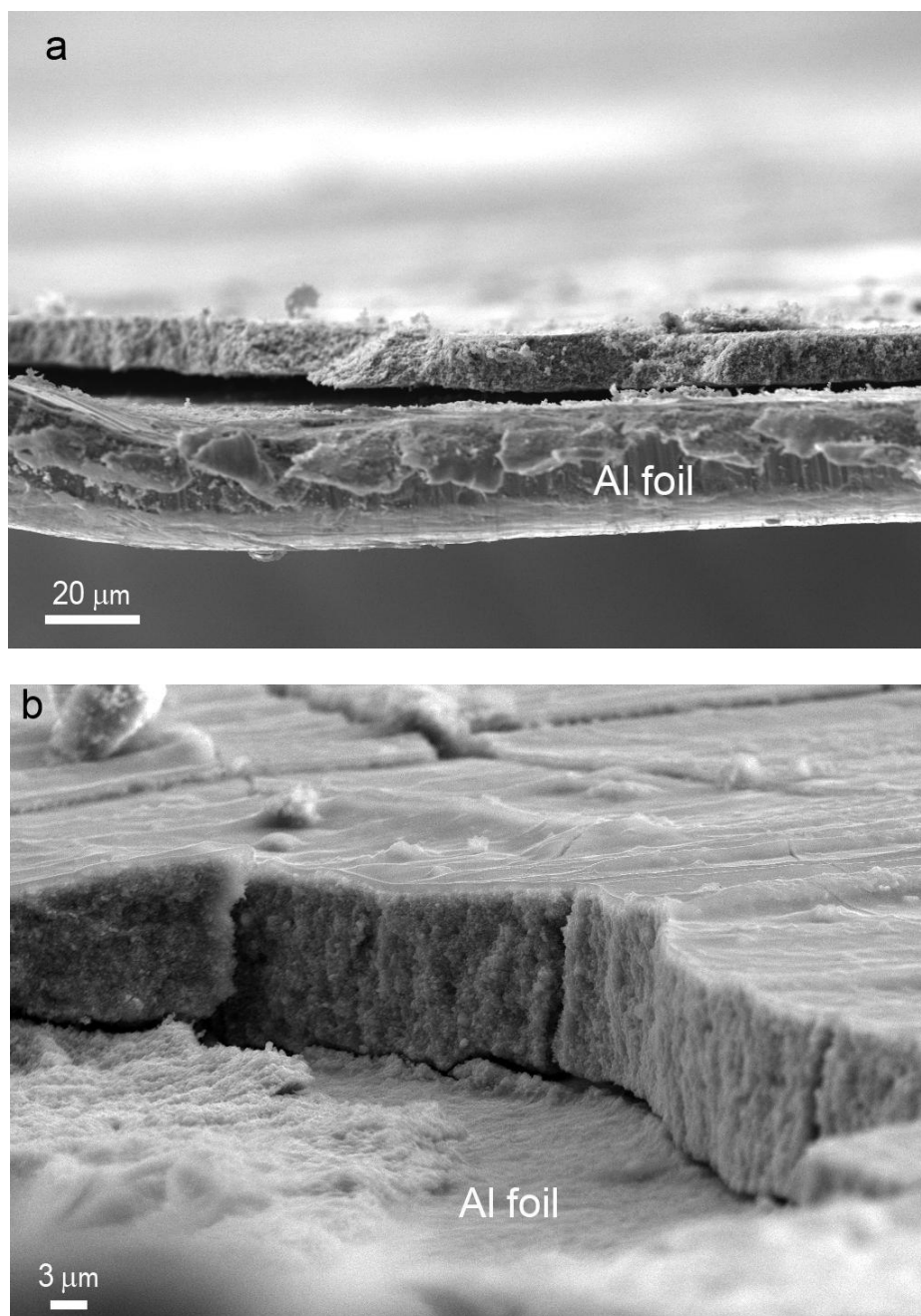
#### 3.1. Characterization of C-LFP and C-LFP/PEDOT:PSS

The XRD patterns of C-LFP material, C-LFP/PEDOT:PSS initial composite and C-LFP/PEDOT:PSS composite after 100 cycles are shown in Fig. 1a,b,c.



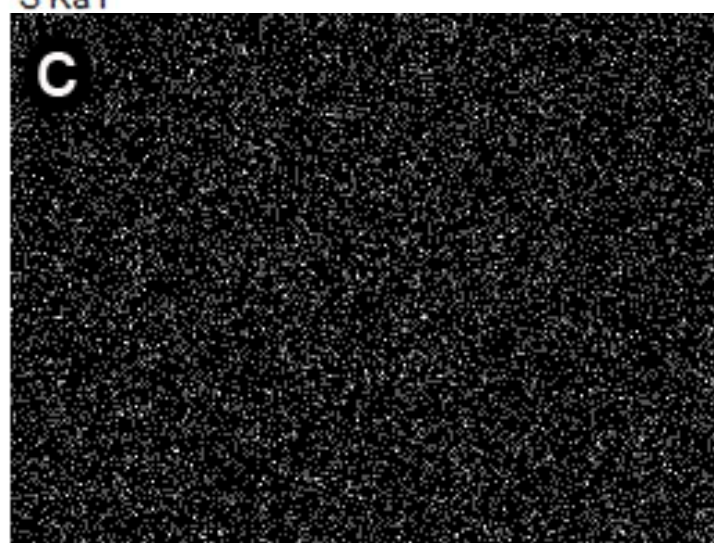
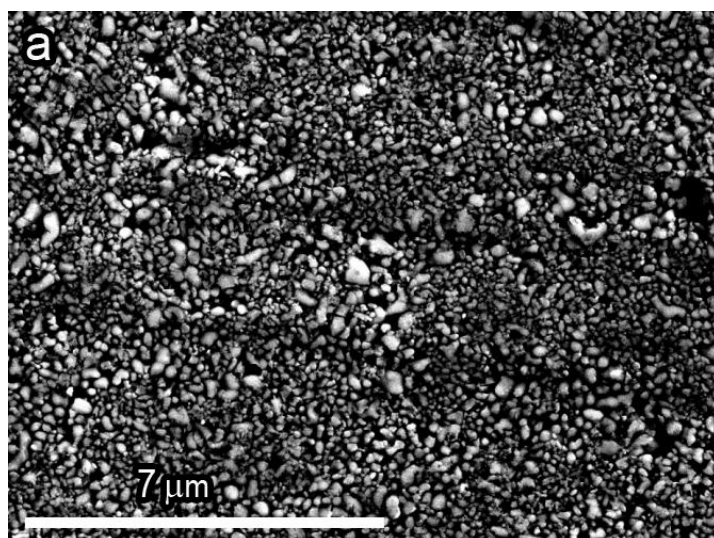
**Figure 1.** XRD patterns of C-LFP pristine material (a), C-LFP/PEDOT:PSS initial composite (b) and C-LFP/PEDOT:PSS composite after 100 cycles (c).

All samples showed well-defined characteristic reflections for the orthorhombic olivine-type structure of LiFePO<sub>4</sub>. After mixing C-LFP with PEDOT:PSS polymer dispersion, no significant changes were observed on XRD patterns (Fig. 1b), the obtained data for initial composite confirmed the maintenance of highly crystalline structure of LFP without any diffraction peaks for PEDOT, probably due to its low content and amorphous nature (all peaks were indexed according to ICDD card No. 01-083-2092). Also there were no detectable carbon diffraction peaks due to the small amount of amorphous carbon in C-LFP. After long-term cycling the composite maintains good crystallinity, as shown by the sharp diffraction peaks indexed according to ICDD card No. 01-072-3571 (Fig. 1c).



**Figure 2.** C-LFP/PEDOT:PSS composite layer on the Al foil, a) before and b) after cycling at 1 C rate for 100 cycles.

SEM images of the C-LFP/PEDOT:PSS electrode layer (Fig. 2) demonstrate the integrity of active layer structure. Recently [32] it was shown that the binding force of PEDOT:PSS was strong enough to obtain coatings with 1 wt.% PEDOT:PSS. It can be seen from Fig. 2a, that PEDOT:PSS acts as a good binder for C-LFP material even at 0.5 wt.% content, forming the compact layer of cathode material and keeping the mechanical integrity of the composite on Al foil current collector. The electrode layer remains consistent even after high stress applied to the edge during the cutting procedure. The SEM image of C-LFP/PEDOT:PSS electrode after 100 charge-discharge cycles at 1 C rate (Fig. 2b) evidences that the film structure remains dense and uniform.



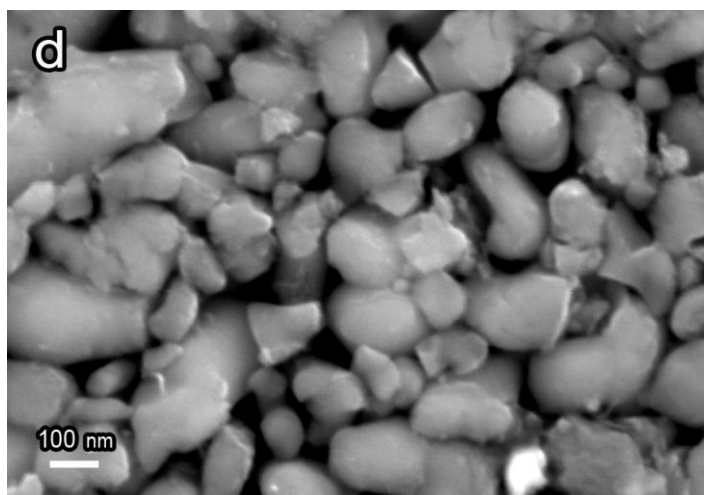


**Figure 3.** Element mapping and high-resolution SEM image of C-LFP/PEDOT:PSS composite; a) image of an area, analyzed by EDX element mapping; b) distribution of sulfur across the electrode area; c) distribution of iron across the electrode area; d) high-resolution image of the electrode surface.

EDX element mapping of the surface of C-LFP/PEDOT:PSS electrode sample was performed for the area visible in Fig.3a and the mapping data are presented in Figs. 3b and 3c. The almost uniform distribution of sulfur, which is the characteristic element of PEDOT, over the electrode surface (Fig. 3b), together with iron from LFP (Fig. 3c) is observed. On the high resolution image (Fig. 3d) it is visible that C-LFP particles are covered with thin PEDOT:PSS layer, which ensures electrical contact between them. The size of LFP particles varies from 50 to 200 nm.

### 3.2. Electrochemical characterization

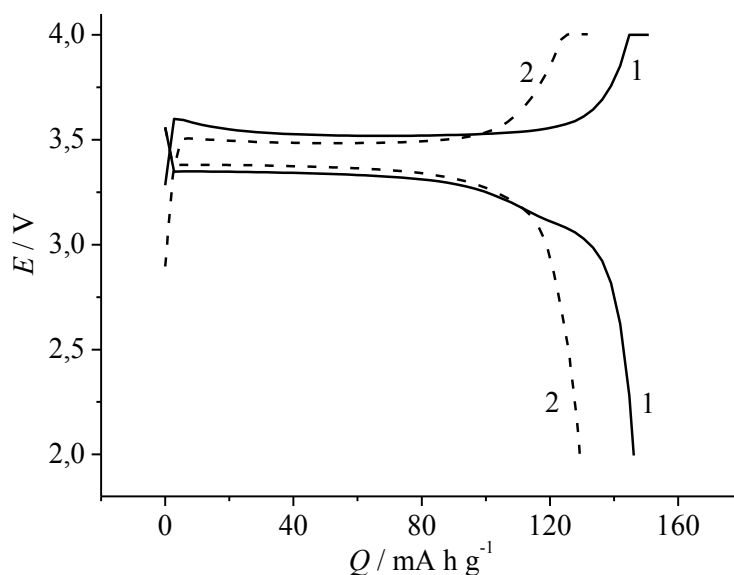


**Figure 4.** Charge-discharge profiles of C-LFP/PEDOT:PSS composite electrode (1) and 84:8:8 wt.% C-LFP/PVDF/C electrode (2). Charge current is 0.2 C and discharge current is 1 C.

Fig. 4 demonstrates the charge-discharge curves of the battery cell with C-LFP/PEDOT:PSS composite electrode, recorded at 0.2 C charge and 1 C discharge rates, in comparison with 84:8:8 wt.% C-LFP/PVDF/C electrode. The discharge specific capacity increased for about 15% after replacement of inactive electrode components with conductive polymer, reaching the value of specific capacity 141 mAh g<sup>-1</sup> (at 1 C). The discharge curve of C-LFP/PEDOT:PSS composite electrode exhibits a characteristic flat plateau at 3.36 V across a large capacity range. The discharge potential plateau of C-LFP/PVDF/C electrode is located at 3.39 V.

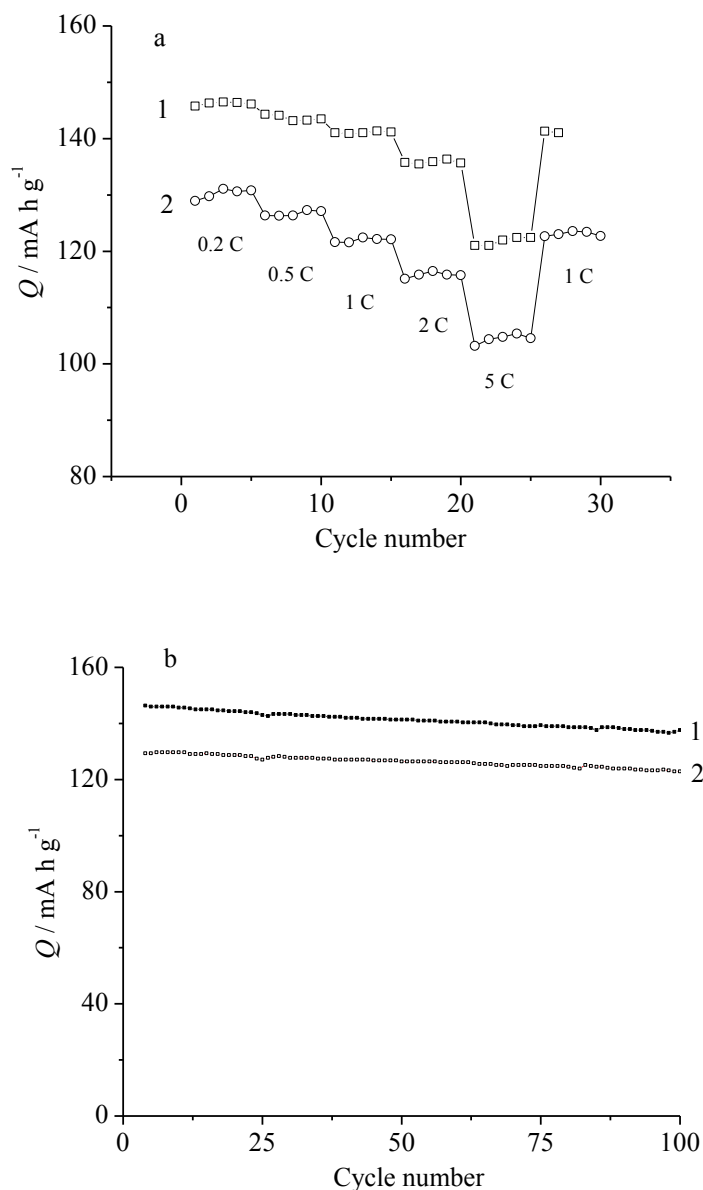


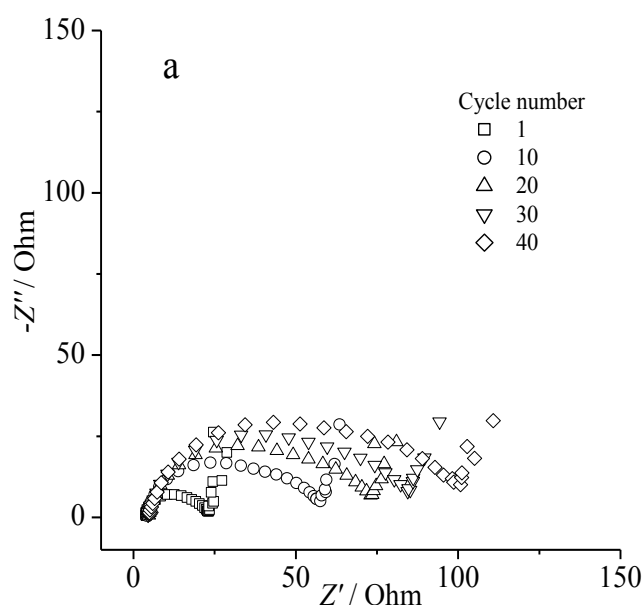
**Figure 5.** a) C-rate capability (charge current 0.2 C, discharge current is presented on the plot) and b) long-term cyclability (at 1 C charge and discharge) of C-LFP/PEDOT:PSS composite electrode (1) and 84:8:8 wt.% C-LFP/PVDF/C electrode (2).



At higher discharge rates, the discharge capacity of C-LFP/PEDOT:PSS electrodes remains higher than the capacity of C-LFP/PVDF/C electrodes even at 5C. Fig. 5a displays electrode discharge capacity as a function of cycle number for C-LFP/PVDF/C and C-LFP/PEDOT:PSS composite, obtained at various current densities from 0.2C to 5C after charging at 0.2 C. For all the current rates studied, the discharge capacity for C-LFP/PEDOT:PSS composite is enhanced for about 20 mAh g<sup>-1</sup> compared with C-LFP/PVDF/C composition, especially at high rates. The capacity reached 147 mAh g<sup>-1</sup> at 0.2 C and 122 mAh g<sup>-1</sup> at 5 C. The capacity returns to the initial value (140 mAh g<sup>-1</sup>) if the discharge current rate is set back to 1C after charge/discharge at various rates. Therefore, the capacity of C-LFP based cathode is greatly improved for discharging at different C-rates with introduction of PEDOT:PSS instead of traditional binders.

Fig. 5b compares discharge capacity vs. cycle number of the C-LFP/PEDOT:PSS composite and C-LFP/PVDF/C materials. The data were obtained by charging and discharging the material at room temperature over 100 cycles at a rate of 1 C. The C-LFP/PEDOT:PSS composite shows higher capacity and similar cyclability as compared to C-LFP/PVDF/C. The battery cells with C-LFP/PEDOT:PSS and C-LFP/PVDF/C materials have almost the same slope of capacity loss with cycle number. Capacity retention was found to be 98% after 100 cycles as compared to the initial value obtained at 1C. This is similar to the value for conventional composition of C-LFP electrode with addition of carbon black and PVDF binder. So, the substitution of all inactive components by only 0.5% of conducting polymer PEDOT:PSS improves the specific capacity of material and maintains the prolonged cycle life.

It is interesting to note that the specific capacitance and rate cyclability of the obtained electrodes are higher than ones of previously described electrodes with PEDOT:PSS contents of 6 wt.% or more [33].



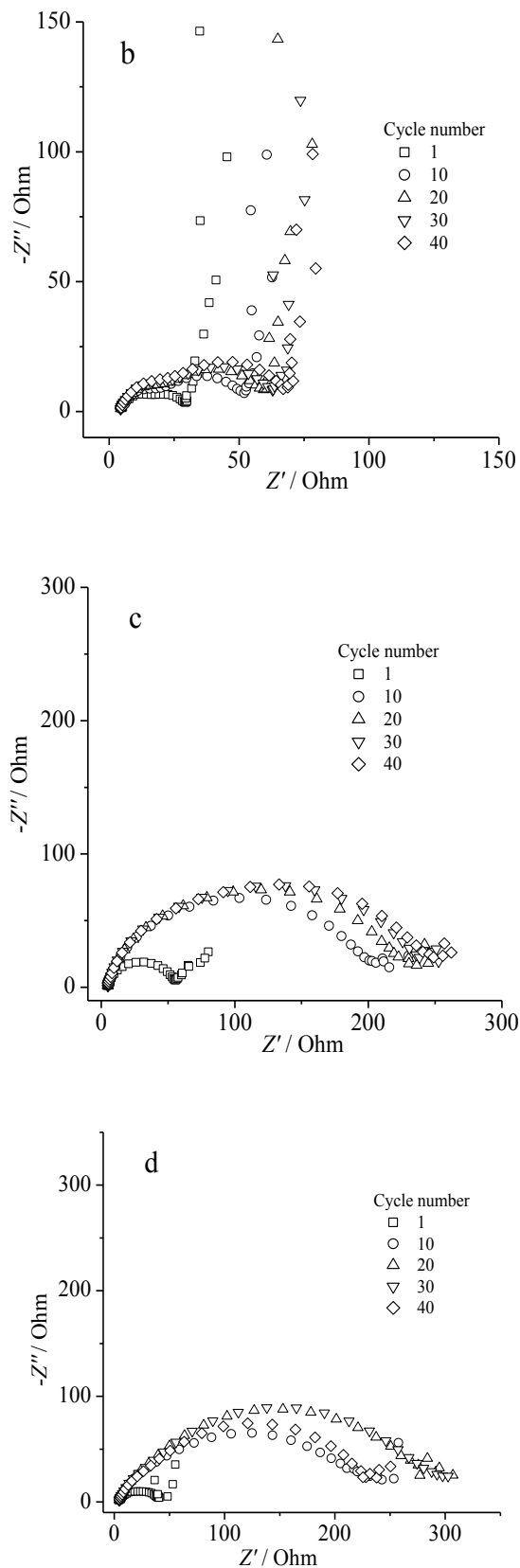


**Figure 6.** EIS spectra of C-LFP/PEDOT:PSS composite (a, c) and 84:8:8 wt.% C-LFP/PVDF/C electrode (b, d), frequency range 100 kHz – 1 Hz. Impedance spectra were recorded in charged (a, b) and discharged (c, d) states of the battery at different cycle numbers.

To explain this, we should remember that electronic and ionic conductivity of PEDOT:PSS polymer is relatively low (comparing with carbon). In this case, high polymer content in the electrode material can lead to formation of thick PEDOT:PSS layers around LFP particles, which may hinder electron and ion transport. On the contrary, if only a small amount of PEDOT:PSS is used, it provides good enough conductive pathway between the particles, but does not block their surface completely, as can be seen from Fig. 3. To check the conductivity of obtained electrodes, impedance spectroscopy was used.

Fig. 6 presents EIS spectra in complex plane for the battery cells with C-LFP/PEDOT:PSS composite (Fig. 6a, c) and conventional C-LFP/PVDF/C cathodes (Fig. 6b, d). Impedance spectra were recorded in charged (Fig. 6a, b) and discharged (Fig. 6c, d) states of the batteries after a series of charge-discharge cycles performed at 1 C rate. The observed impedance spectra are typical for lithium-ion battery cells.  $Z'$ ,  $-Z''$  dependencies are composed of a depressed semicircle in high frequency region and a straight line that is observed in low frequency region. An intercept of  $Z'$ ,  $-Z''$  curves with real impedance axis at high frequency limit corresponds to the ohmic resistance of electrolyte. Diameter of semicircle shows the charge transfer resistance that is related to complex charge transfer process between electrolyte and active electrode material in the composite electrode. The values of  $R_{ct}$  for the first discharge cycle are 55 Ohms for C-LFP/PEDOT:PSS composite electrodes and 41 Ohms for C-LFP/PVDF/C electrode. During further cycling for both types of cells  $R_{ct}$  increases up to 200-300 Ohms and remains in this range. The values of  $R_{ct}$  obtained from impedance spectra recorded in the charged state of the battery for the first discharge cycle are 23 Ohms for C-LFP/PEDOT:PSS composite and 30 Ohms for C-LFP/PVDF/C cathode, then  $R_{ct}$  increases and remains in the range of 50-100 Ohms during all further cycling for both types of cells.

According to the impedance data, C-LFP/PEDOT:PSS composite electrode and conventional C-LFP/PVDF/C electrode have comparable values of the charge transfer resistances. It can be observed that the increase of the charge transfer resistance with prolonged cycling depends mostly on the LFP material itself, and is not affected by the electrode composition.

The goal of our study was to propose the new slurry composition by replacement of traditional binders and conductive additives, which allowed increasing the content of active components in the electrode material. As a result, we can conclude that the proposed new slurry composition allows to obtain cathodes with capacity increased by 15% compared to the traditional ones and preserve other important parameters such as internal resistance or cyclability on the same level.

It is also worth to compare our findings with the state-of-art researches on the similar topic. In this case, it is reasonable to compare the capacities of the electrodes referring to the electrode mass (excluding current collector). At the same time, most authors present their data normalized by the active mass, i.e. by  $\text{LiFePO}_4$  mass. Therefore, for some cases we had to recalculate given capacity values of composite electrodes, referring them to the electrode mass. According to the concept of our study, we have limited our analysis by the papers, discussing new compositions with conductive polymer PEDOT and PEDOT:PSS additives combined with commercial LFP, and other additives allowing to reduce the content of non-electroactive components in cathode material. Results of performed analysis are summarized in the Table 1.

One can see from the Table 1 that specific capacities of electrodes obtained in this study, referring to electrode mass, are 10% or higher than reported by different authors. It means that the proposed approach is one of the most efficient methods of increasing the practical battery capacity, providing more than 10% energy density gain compared to other known modifications of LFP cathode material. In addition, it seems that the electrode preparation procedure described here is simple enough to be scaled for mass production level.

**Table 1.** Specific capacity values for different electrode compositions

LiFePO <sub>4</sub> content, wt. %	Binder		Conductive additives		Capacitance at 1 C rate** discharge at room temperature, mAh g <sup>-1</sup>		Reference
	material	content, wt. %	material	content, wt. %	normalized by active mass	normalized by electrode mass	
99.5	PEDOT:PSS	0.5	* PEDOT:PSS acts also as a conducting additive		142	141	this study
84	PVDF	10	carbon black	10	146	123	this study
90	Carboxymethyl chitosan/Styrene- butadiene rubber	8	carbon black	8	141	127	[34]
90	Carboxymethyl cellulose	4	carbon black	6	129	116	
80	PVDF	10	carbon black	10	144	115	
94	PEDOT:PSS	6	* PEDOT:PSS acts also as a conducting additive		103	97	
92	PEDOT:PSS	8	* PEDOT:PSS acts also as a conducting additive		117	108	[33]
84	PEDOT:PSS	16	* PEDOT:PSS acts also as a conducting additive		75	63	
84	PVDF	6	carbon black	10	120	101	
85	PVDF	7	carbon black	8	71	60	[26]
80	PEDOT	20	carbon black	0	98	78	[26]
85	PVDF	7	carbon black	8	71	60	[26]
80	PVDF	10	Super P	10	119	95	[35]
80	PMMA	10	Super P	10	111	89	[35]
80	PVDF-HFP	10	Super P	10	126	101	[35]
85 (LFP/C)	PVDF	7	carbon black	8	90	77	[27]
85% (LFP/C)	0.3mg PEDOT:PSS was cast over electrode with composition 85% (LFP/C): 7%PVDF: 4% carbon black				80	68	[27]
75	PTFE	5	carbon black	20	160	120	[36]
75 (LFP+PANI)	PTFE	5	carbon black	20	171	128	[36]
75	PVA	12.5	Super P	12.5	149	112	[37]
80	CMC-Li	10	acetylene black	10	139	111	[38]
94	PEDOT	6	no	0	82	77	[33]
92	PEDOT	8	no	0	115	106	[33]

84	PEDOT	16	no	0	77	65	[33]
84	PVDF	6	carbon black	10	107	90	[33]
33.5	PEDOT 66.5%				160 (0.1C)	75 (0.1C)	[19]
75	PTFE	5	PEDOT doped by p-TSA (p-toluene sulfonic acid)	20	140	113	[17]
84.5	PVDF	7.5	PEDOT	8	151	128	[21]

\* PEDOT:PSS plays a dual role as a binder and conductor

\*\* if not stated otherwise

#### 4. CONCLUSIONS

The effect of replacement of carbon black and PVDF binder by small amount of PEDOT:PSS polymer dispersion in C-LFP-based cathode was investigated. Composite cathode material C-LFP/PEDOT:PSS with high content of active C-LFP material (99.5 wt.%) was prepared by technologically simple mechanical mixing of C-LFP and commercially available PEDOT:PSS dispersion. It was shown that introduction of small amount of PEDOT:PSS (0.5 wt.%) instead of conventional content of inactive carbon black and binder allows to reduce significantly the inactive mass (up to 15%) and increase the specific gravimetric capacity ( $147 \text{ mAhg}^{-1}$  at 0.2 C). Introduction of PEDOT:PSS also enhances the rate capability of composite electrodes, preserving stable cycle life and good reversibility of charge-discharge processes. According to our data and literature data, found for other PEDOT:PSS-bound electrodes with higher polymer contents, the proposed composition demonstrates the best performance, because the even 0.5 wt.% amount of the conductive polymer forms enough conductive pathway between particles. The obtained SEM images of the composite material along with electrochemical experimental data demonstrate that PEDOT:PSS can serve as a good binder, providing the morphological integrity of material during prolonged charge/discharge cycling. Comparison of electrochemical performance of conventional C-LFP/PVDF/C electrode and C-LFP/PEDOT:PSS composite electrode allows to consider the later as a possible cathode material for lithium ion batteries. Further studies of optimal C-LFP/PEDOT:PSS composite electrodes are in progress.

#### ACKNOWLEDGMENTS

The financial support from the Russian Foundation for Basic Research (grant № 14-29-04043) is gratefully acknowledged. The authors would like to thank the Nanotechnology Interdisciplinary Centre and the Centre for X-ray Diffraction Studies of Saint-Petersburg State University Research Park for providing common SEM, EDX and XRD analysis.

#### References

1. A.K. Padhi, K.S. Nanjundaswamy and J.B. Goodenough, *J. Electrochem. Soc.*, 144 (1997) 1188
2. L.X. Yuan, Z.H. Wang, W.X. Zhang, X.L. Hu, J.T. Chen, Y.H. Huang and J.B. Goodenough, *Energy Environ. Sci.*, 4 (2011) 269

3. K. Zaghib, A. Mauger and C.M. Julien, *J. Solid State Electrochem.*, 16 (2012) 835
4. P. Bruce, B. Scrosati and J.M. Tarascon, *Angew. Chem. Int. Ed.*, 47 (2008) 2930
5. S. Franger, F. Le Cras, C. Bourbon and H. Rouault, *Electrochem. Solid State Lett.*, 5 (2002) A231
6. P.P. Prosini, M. Carewska, S. Scaccia, P. Wisniewski, S. Passerini and M. Pasquali, *Electrochim. Acta*, 48 (2003) 4205
7. N. Ravet, Y. Chouinard, J.F. Magnan, S. Besner, M. Gauthier and M. Armand, *J. Power Sources*, 97-98 (2001) 503
8. Y.H. Huang, K.S. Park and J.B. Goodenough, *J. Electrochem. Soc.*, 153 (2006) A2282
9. G.X. Wang, L. Yang, S.L. Bewlay, Y. Chen, H.K. Liu and J.H. Ahn, *J. Power Sources*, 146 (2005) 521
10. H.C. Shin, W.I. Cho and H. Jang, *Electrochim. Acta*, 52 (2006) 1472
11. G.X. Wang, S. Bewlay, J. Yao, J.H. Ahn, H.K. Liu and S.X. Dou, *Electrochem. Solid State Lett.*, 7 (2004) A503
12. S.Y. Chung, J.T. Bloking and Y.M. Chiang, *Nat. Mater.*, 1 (2002) 123
13. D. Wang, H. Li, S. Shi, X. Huang and L. Chen, *Electrochim. Acta*, 50 (2005) 2955
14. F. Croce, A.D. Epifanio, J. Hassoun, A. Deptula, T. Olczac and B. Scrosati, *Electrochem. Solid State Lett.*, 5 (2002) A47
15. K.S. Park, J.T. Son, H.T. Chung, S.J. Kim, C.H. Lee, K.T. Kang and H.G. Kim, *Solid State Commun.*, 129 (2004) 311
16. K.S. Park, S.B. Schougaard and J.B. Goodenough, *Adv. Mater.*, 191 (2007) 848
17. A. Vadivel Murugan, T. Muraliganth and A. Manthiram, *Electrochem. Commun.*, 10 (2008) 903
18. I. Boyano, J.A. Blazquez, I. de Meatza, M. Bengoechea, O. Miguel, H. Grande, Y.H. Huang and J.B. Goodenough, *J. Power Sources*, 195 (2010) 5351
19. N.D. Trinh, M. Saulnier, D. Lepage and S.B. Schougaard, *J. Power Sources*, 221 (2013) 284
20. G. X. Wang, L. Yang, Y. Chen, J. Z. Wang, S. Bewlay and H. K. Liu, *Electrochim. Acta*, 50 (2005) 4649
21. D. Lepage, C. Michot, G. Liang, M. Gauthier and S.B. Schougaard, *Angew. Chem. Int. Ed.*, 50 (2011) 6884
22. W.-M. Chen, Y.-H. Huang and L.-X. Yuan, *J. Electroanal. Chem.*, 660 (2011) 108
23. W.-M. Chen, L. Qie, L.-X. Yuan, S.-A. Xia, X.-L. Hu, W.-X. Zhang and Y.-H. Huang, *Electrochim. Acta*, 56 (2011) 2689
24. J.K. Kim, J. Manuel, M.H. Lee, J. Scheers, D.H. Lim, P. Johansson, J.H. Ahn, A. Matic and P. Jacobsson, *J. Mater. Chem.*, 22 (2012) 15045
25. R. Holze and Y.P. Wu, *Electrochim. Acta*, 122 (2014) 93
26. D. Cintora-Juarez, C. Perez-Vicente, S. Ahmad and J.L. Tirado, *RSC Advances*, 4 (2014) 26108
27. N. Vicente, M. Haro, D. Cíntora-Juárez, C. Pérez-Vicente, J.L. Tirado, S. Ahmad and G. Garcia-Belmonte, *Electrochim. Acta*, 163 (2015) 323
28. L. Zhan, Z. Song, J. Zhang, J. Tang, H. Zhan, Y. Zhou and C. Zhan, *Electrochim. Acta*, 53 (2008) 8319
29. H.-C. Dinh, S.-I. Mho and I.-H. Yeo, *Electroanalysis*, 23 (2011) 2079
30. H.-C. Dinh, I.-H. Yeo, W.I. Cho and S.-I. Mho, *ECS Trans.*, 28 (2010) 167
31. J.M. Kim, H.S. Park, J.H. Park, T.H. Kim, H.K. Song and S.Y. Lee, *ACS Appl. Mater. Inter.*, 6 (2014) 12789
32. J. Kim, H.S. Park, T.H. Kim, S.Y. Kim and H.K. Song, *Phys. Chem. Chem. Phys.*, 16 (2014) 5295
33. P.R. Das, L. Komsysiaka, O. Ostera and G. Wittstock, *J. Electrochem. Soc.*, 162 (2015) A674
34. M. Sun, H. Zhong, S. Jiao, H. Shao and L. Zhang, *Electrochim. Acta*, 127 (2014) 239.
35. S. Hu, Y. Li, J. Yin, H. Wang, X. Yuan and Q. Li, *Chemical Engineering Journal*, 237 (2014) 497.
36. W.M. Chen, L. Qie, L.-X. Yuan, S.-A. Xia, X.-L. Hu, W.-X. Zhang and Y.-H. Huang, *Electrochim. Acta*, 56 (2011) 2689.
37. P.P. Prosini, C. Cento, M. Carewska and A. Masci, *Solid State Ionics*, 274 (2015) 34.

38. L.Qiu, Z. Shao, D. Wang, F. Wang, W. Wang and J. Wang, *Carbohydrate Polymers*, 112 (2014) 532.

© 2015 The Authors. Published by ESG ([www.electrochemsci.org](http://www.electrochemsci.org)). This article is an open access article distributed under the terms and conditions of the Creative Commons Attribution license (<http://creativecommons.org/licenses/by/4.0/>).